Halogenated $La_{1.6}Sr_{0.4}CuO_4$ catalysts active for ethane selective oxidation to ethene

H.X. Dai, C.F. Ng and C.T. Au *

Department of Chemistry and Center for Surface Analysis and Research, Hon Kong Baptist University, Kowloon Tong, Hong Kong, PR China
E-mail: pctau@hkbu.edu.hk

Received 9 February 2000; accepted 11 May 2000

The catalytic performances and characterization of the catalysts $La_{1.6}Sr_{0.4}CuO_{3.852}$, $La_{1.6}Sr_{0.4}CuO_{3.857}F_{0.143}$, and $La_{1.6}Sr_{0.4}CuO_{3.856}Cl_{0.126}$ have been investigated for the oxidative dehydrogenation of ethane (ODE) to ethene. X-ray diffraction results indicated that the three catalysts have a single-phase tetragonal K_2NiF_4-type structure. The incorporation of fluoride or chloride ions in the $La_{1.6}Sr_{0.4}CuO_{4-\delta}$ lattice can significantly enhance C_2H_6 conversion and C_2H_4 selectivity. We observed 83.2% C_2H_6 conversion, 76.7% C_2H_4 selectivity, and 63.8% C_2H_4 yield over $La_{1.6}Sr_{0.4}CuO_{3.857}F_{0.143}$ and 79.6% C_2H_6 conversion, 74.6% C_2H_4 selectivity, and 59.4% C_2H_4 yield over $La_{1.6}Sr_{0.4}CuO_{3.856}Cl_{0.126}$ under the reaction conditions of $C_2H_6/O_2/N_2$ molar ratio 2/1/3.7, temperature 660 °C, and space velocity 6000 ml h^{-1} g^{-1}. With the rise in space velocity, C_2H_6 conversion decreased, whereas C_2H_4 selectivity increased. Life studies showed that the two catalysts were durable within 60 h of on-stream ODE reaction. Based on the results of X-ray photoelectron spectroscopy, O_2 temperature-programmed desorption, and C_2H_6 and $C_2H_6/O_2/N_2$ (2/1/3.7 molar ratio) pulse studies, we conclude that (i) the inclusion of halide ions in the $La_{1.6}Sr_{0.4}CuO_{4-\delta}$ lattice could promote lattice oxygen mobility, and (ii) the O^- species accommodated in oxygen vacancies and desorbed below 600 °C favor ethane complete oxidation whereas the lattice oxygen species desorbed in the 600–700 °C range are active for ethane selective oxidation to ethene. By regulating the oxygen vacancy density and Cu^{3+}/Cu ratio in the K_2NiF_4-type halo-oxide catalyst, one can generate a durable catalyst with good performance for the ODE reaction.

Keywords: ethane oxidative dehydrogenation, C_2H_4 generation, ODE reaction, K_2NiF_4-type halo-oxide catalyst, $La_{1.6}Sr_{0.4}CuO_{4-\delta}X_\sigma$ (X = F, Cl), XPS characterization, superconducting cuprate material

1. Introduction

Ethane is the second largest component of natural gas and one of the main products in the oxidative coupling of methane (OCM). It is of significance to convert ethane to ethene since ethene is the starting material for synthesizing many value-added chemicals such as polyethylene, polyvinyl chloride, styrene, etc. In the past decades, the oxidative dehydrogenation of ethane (ODE) to ethene has been investigated intensively and extensively. Many compounds have been used as catalysts for this reaction. Among them, $Dy_2O_3/Li^+-MgO-Cl^-$ (ca. 57% C_2H_4 yield at 570 °C) [1], Mo–V–Nb–Sb–Ca–O (ca. 52% C_2H_4 yield at 400 °C) [2], and LiCl/sulfated zirconia (ca. 68% C_2H_4 yield at 650 °C) [3] seem to be highly effective. Although $KSr_2Bi_3O_4Cl_6$ [4], a layered complex compound, gave a C_2H_4 yield of ca. 70% at 640 °C, the catalyst deteriorated due to Cl leaching. In recent years, many researchers have reported that perovskite-type oxides such as $SrCo_{0.8}Li_{0.2}O_3$ [5], $SrCo_{0.8}Fe_{0.2}O_3$ and $La_{0.8}Sr_{0.2}CoO_3$ [6], $CaCo_{0.8}Fe_{0.2}O_3$ [7], and $La_{0.6}Sr_{0.4}Co_{0.8}Fe_{0.2}O_3$ [8] displayed moderate catalytic performance for the OCM reaction. More recently, after investigating a series of $La_{1-x}Sr_xFeO_{3-\delta}$ catalysts, Yi et al. [9] found that $SrFeO_{3-\delta}$ showed 87% C_2H_6 conversion and 43% C_2H_4 selectivity with 37% C_2H_4 yield under the reaction conditions: temperature 650 °C, C_2H_6/O_2 molar ratio 1/1, and space velocity ca. 7000 ml h^{-1} g^{-1}.

Perovskite materials are known to be active for the total oxidation of carbon monoxide and hydrocarbons [10,11]. The oxygen vacancies and redox properties of these catalysts play important roles in the catalysis of the complete oxidation reactions. Generally speaking, a perovskite-type oxide catalyst with higher oxygen vacancy density and stronger redox ability performs better. If one could decrease the oxygen vacancy density and strengthen the redox ability by incorporating halide ions (which have ionic radii similar to O^{2-} ions) to the oxygen vacancies, one would convert these combustion materials to catalysts selective for the oxidation of ethane to ethene. Based on this idea, we have generated several classes of halide-doped perovskite-type and perovskite-related (K_2NiF_4-type) oxide catalysts. In our previous studies, we have characterized and reported $La_{1-x}Sr_xFeO_{3-\delta}X_\sigma$ (X = F, Cl) [12] and $SrFeO_{3-\delta}Cl_\sigma$ [13] catalysts, which showed good activity and durability for the ODE reaction. Since the discovery of hole-doped, high-temperature superconductivity (HTSC) materials $La_2CuO_{4-\delta}$ [14], a large number of works concerning $La_{2-x}A_xCuO_{4-\delta}$ (A = Sr, Ba) [15,16] as well as fluorinated $La_2CuO_{4-\delta}$ [17–23] and fluorinated $La_{2-x}Sr_xCuO_{4-\delta}$ [24] have been reported, most of which focused on the investigation of physical properties such as

* To whom correspondence should be addressed.

crystal structure, magnetic nature, electric conductivity, and oxygen nonstoichiometry [15–28]. In recent years, Swamy and coworkers [29,30] studied the catalytic decomposition of nitrous oxide on $La_2CuO_{4-\delta}$ and $La_{2-x}Sr_xCuO_{4-\delta}$ and they attributed the high activity of these catalysts to the presence of oxygen vacancies and copper in a mixed oxidation state (Cu^{2+} and Cu^{3+}). Nguyen et al. [31] reported that in the solid oxide solution of $La_{2-x}Sr_xCuO_{4-\delta}$, maximal Cu^{3+} concentration was observed at a Sr-substituted amount of $x = 0.33$. By employing $La_{2-x}Sr_xCuO_{4-\delta}$ as catalyst for the complete oxidation of carbon monoxide, Rajadurai et al. [32] found that the catalytic activity shows a "volcano" behavior with a maximum activity at $x = 0.4$; they interpreted the feature to be due to positive holes (Cu^{3+}), which may provide a favorable environment for the adsorption of CO and O_2 in CO oxidation. The chemical properties, especially catalytic behaviours of halogenated materials, however, have not been well studied. In the present study, we report the catalytic performances and characterization of K_2NiF_4-type halo-oxide $La_{1.6}Sr_{0.4}CuO_{4-\delta}X_\sigma$ (X = F, Cl) as well as $La_{1.6}Sr_{0.4}CuO_{4-\delta}$ (for comparison purposes) for the partial oxidation of ethane to ethene.

2. Experimental

The $La_{1.6}Sr_{0.4}CuO_{4-\delta}$ catalyst was prepared by adopting the method of citric acid complexing [33]. $La(NO_3)_3{\cdot}6H_2O$ (Acros, >99%), $Sr(NO_3)_2$ (Fluka, >99%), and $Cu(C_2H_3O_2)_2{\cdot}H_2O$ (Sigma, >98%) were mixed in aqueous solution at the desired stoichiometric ratio. Citric acid (Aldrich, >99%) equimolar to the metals was added. The solution was then evaporated at 70 °C to produce a viscous syrup. After subsequent evaporation at 120 °C for 8 h and calcination at 1030 °C in oxygen for 24 h, the material was ground. The fluorination or chlorination of $La_{1.6}Sr_{0.4}CuO_{4-\delta}$ was carried out in a vacuum (0.1 Torr) furnace first at 350 °C for 10 h and then at 630 °C for 15 h by using NH_4F or NH_4Cl as a halogenating reagent [34]. After halogenation, the samples were quenched to room temperature and were in turn ground, tabletted, crushed, and sieved to a size range of 80–100 mesh.

The testing of catalytic activity was performed at atmospheric pressure with 0.5 g of the catalyst being dispersed in 5.0 g quartz sand in a fixed-bed quartz microreactor (i.d. = 4 mm). The flow rate was 14.8 ml min^{-1} for ethane and 35.2 ml min^{-1} for air, giving a $C_2H_6/O_2/N_2$ molar ratio of 2/1/3.7 and a space velocity of 6000 ml h^{-1} g^{-1}. The product mixture (C_2H_6, C_2H_4, CH_4, CO, and CO_2) was analyzed on-line by a gas chromatograph (Shimadzu 8A TCD) with Porapak Q and 5A Molecular Sieve columns. The balances of carbon and oxygen were estimated to be 100 ± 2 and 100 ± 3%, respectively, for every run over the catalysts.

The crystal phases of the catalysts were determined by an X-ray diffractometer (XRD, D-MAX, Rigaku) operating at 40 kV and 200 mA using Cu K_α radiation. The patterns recorded were referred to the powder diffraction files – PDF-2 database for the identification of crystal structures. X-ray photoelectron spectroscopy (XPS, Leybold Heraeus-Shengyang SKL-12, VG CLAM 4 MCD analyser) was used to determine the O(1s) binding energy of surface oxygen species. Before XPS measurements, the samples were calcined in O_2 (flow rate 20 ml min^{-1}) at 800 °C for 1 h and then cooled in O_2 to room temperature, followed by treatments in He (20 ml min^{-1}) at 400, 580, and 680 °C for 1 h, respectively, and then cooling in He to room temperature. The treated samples were then outgassed in the primary vacuum chamber at 10^{-5} Torr for 0.5 h and then introduced into the ultrahigh vacuum chamber for recording. The C(1s) line at 284.6 eV was taken as a reference for binding energy calibration. The specific surface areas of the catalysts were measured using the BET method on a Nova 1200 apparatus.

In order to study the variations of oxidation state of copper ions after the desorption of oxygen species, we treated the samples (0.5 g) in He (20 ml min^{-1}) or in oxygen (20 ml min^{-1}) at various temperatures for 30 min and then cooled them down in the same atmosphere to room temperature, respectively.

The O_2-TPD (temperature-programmed desorption) and TGA (thermogravimetric analysis) experiments were performed according to the methods described previously [12]. The amount of O_2 desorbed from the catalysts was quantified by calibrating the peak areas against that of a standard pulse. In the TGA studies, ca. 20 mg of the sample was used and the temperature range was from room temperature to 720 °C.

We performed pulse experiments to investigate the reactivity of surface oxygen species. A catalyst sample (0.5 g) was placed in a microreactor and was thermally treated at a desired temperature for 30 min before the pulsing of C_2H_6 or $C_2H_6/O_2/N_2$ (2/1/3.7 molar ratio) and the effluent was analyzed on-line by a mass spectrometer. The pulse size was 65.7 μl (at 25 °C, 1 atm) and He (HKO Co., purity >99.995%) was the carrier gas.

The fluorine and chlorine contents in the catalysts were analyzed according to the approach described in [35]. The experimental error for halide analysis is ±0.05%. The methods for the titrimetric analysis of copper oxidation states in the catalysts were: (i) for Cu^{3+} determination, the sample was dissolved in 2.6 M H_3PO_4 solution containing excessive standard 0.1 M Fe^{2+} under an inert atmosphere and the Fe^{2+} remaining after the completion of the reaction $Cu^{3+} + Fe^{2+} \rightarrow Cu^{2+} + Fe^{3+}$ was titrated against standard potassium dichromate [36]; (ii) for Cu^+ determination, the sample was digested in 2.6 M H_3PO_4 solution containing standard 0.1 M Fe^{3+} solution, the Fe^{2+} generated in the reaction $Cu^+ + Fe^{3+} \rightarrow Cu^{2+} + Fe^{2+}$ was titrated against standard potassium dichromate [37]. The experimental errors for Cu^{3+} and Cu^+ content determinations are estimated to be ±0.5%.

Table 1
Crystal structures, compositions, and surface areas of catalysts.

Catalyst	Crystal phase	Cu^{3+}/Cu[a] (mol%)	F or Cl content[b] (wt%)	δ	σ	Surface area[b] ($m^2\,g^{-1}$)
$La_{1.6}Sr_{0.4}CuO_{4-\delta}$	Tetragonal	20.8	–	0.148	–	1.66
$La_{1.6}Sr_{0.4}CuO_{4-\delta}F_\sigma$	Tetragonal	25.8	0.71	0.143	0.143	1.54
			(0.72)			(1.52)
$La_{1.6}Sr_{0.4}CuO_{4-\delta}Cl_\sigma$	Tetragonal	23.8	1.15	0.144	0.126	1.49
			(1.14)			(1.48)

[a] Cu^{3+}/Cu values were calculated based on the assumption that only Cu^{2+} and Cu^{3+} ions are present in the samples.
[b] Data in parentheses were obtained after 60 h of on-stream ODE reaction.

3. Results and discussion

3.1. Catalyst structures, compositions, and catalytic performance

Table 1 summarizes the crystal phases, compositions, and surface areas of $La_{1.6}Sr_{0.4}CuO_{4-\delta}$ and $La_{1.6}Sr_{0.4}CuO_{4-\delta}X_\sigma$. Based on the halide contents and Cu^{3+}/Cu ratios as well as the assumption of electroneutrality, the value of δ was estimated to be 0.148 for $La_{1.6}Sr_{0.4}CuO_{4-\delta}$, whereas δ and σ values were 0.143 and 0.143 for $La_{1.6}Sr_{0.4}CuO_{4-\delta}F_\sigma$, and 0.144 and 0.126 for $La_{1.6}Sr_{0.4}CuO_{4-\delta}Cl_\sigma$, respectively. By comparing the XRD results with the JCPDS data (Nos. 38-1427 and 39-1190), we deduced that the $La_{1.6}Sr_{0.4}CuO_{3.852}$ and $La_{1.6}Sr_{0.4}CuO_{4-\delta}X_\sigma$ catalysts adopted a tetragonal K_2NiF_4-type structure (space group I4/mmm). The single-phase tetragonal structure of the fluorinated or chlorinated material confirms that the halide ions were incorporated into the $La_{1.6}Sr_{0.4}CuO_{4-\delta}$ lattice. The x value of Sr substitution for La could be up to 1.3 while the basic tetragonal structure is maintained by increasing the oxygen vacancies [38]. The introduction of halide ions in limited amount did not induce phase transformation. From table 1, one can realize that the inclusion of halide ions in the $La_{1.6}Sr_{0.4}CuO_{4-\delta}$ lattice has caused the Cu^{3+}/Cu ratio to rise and the oxygen vacancy density to decrease; the addition of halide ions to $La_{1.6}Sr_{0.4}CuO_{4-\delta}$, however, did not bring about any significant change in surface area. It should be noted that according to the results of titration experiments, there were no Cu^+ ions in all the samples.

In a blank experiment, 5.0 g of quartz sand gave a C_2H_6 conversion of 7.6%, a C_2H_4 selectivity of 89.2%, and a C_2H_4 yield of 6.8% at 680 °C. It indicates that quartz sand is poor in catalytic activity. Figure 1 shows the catalytic performances of $La_{1.6}Sr_{0.4}CuO_{3.852}$ and $La_{1.6}Sr_{0.4}CuO_{4-\delta}X_\sigma$ at temperatures ranging from 500 to 680 °C. With the increase in reaction temperature, C_2H_6 and O_2 conversions, C_2H_4 selectivity, and C_2H_4 yield increased whereas CO_x selectivity decreased over $La_{1.6}Sr_{0.4}CuO_{3.852}$. The highest C_2H_4 selectivity (34.4%) was observed at 680 °C; with a C_2H_6 conversion of 33.6%, the C_2H_4 yield was 11.6%. No CH_4 was detected within the temperature range. With the increase in temperature from 500 to 680 °C over the $La_{1.6}Sr_{0.4}CuO_{3.857}F_{0.143}$ catalyst, C_2H_6 and O_2 conversions

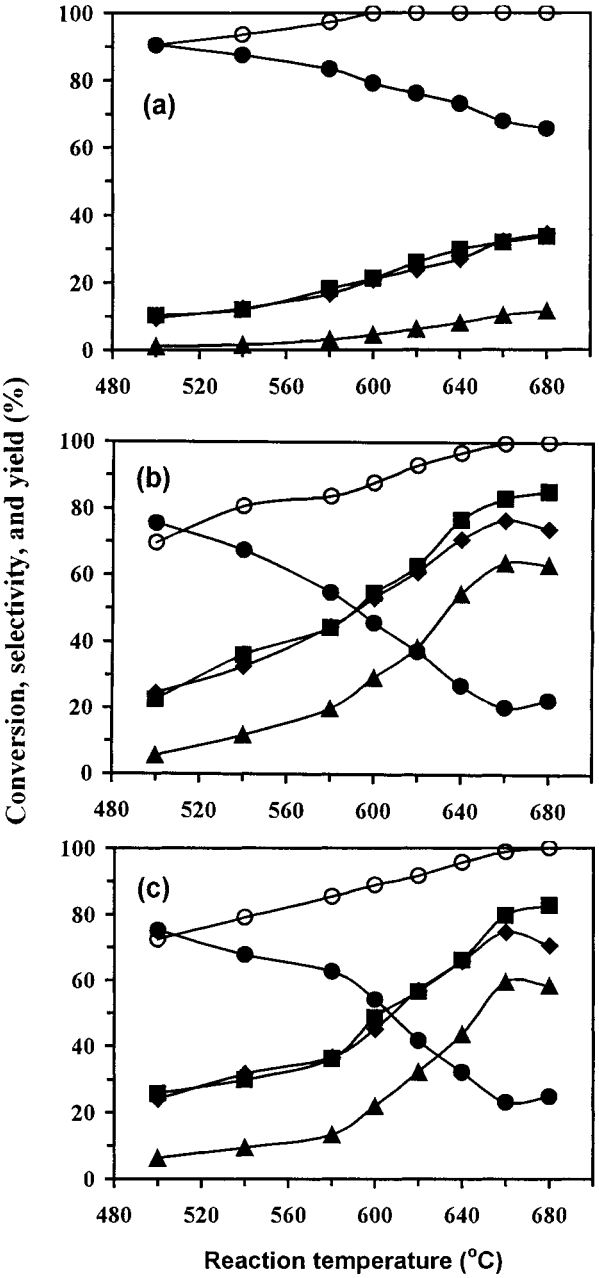

Figure 1. Catalytic performance of (a) $La_{1.6}Sr_{0.4}CuO_{3.852}$, (b) $La_{1.6}Sr_{0.4}CuO_{3.857}F_{0.143}$, and (c) $La_{1.6}Sr_{0.4}CuO_{3.856}Cl_{0.126}$ as related to reaction temperature at 6000 ml $h^{-1}g^{-1}$. (■) C_2H_6 conversion, (♦) C_2H_4 selectivity, (▲) C_2H_4 yield, (●) CO_x selectivity, (○) O_2 conversion.

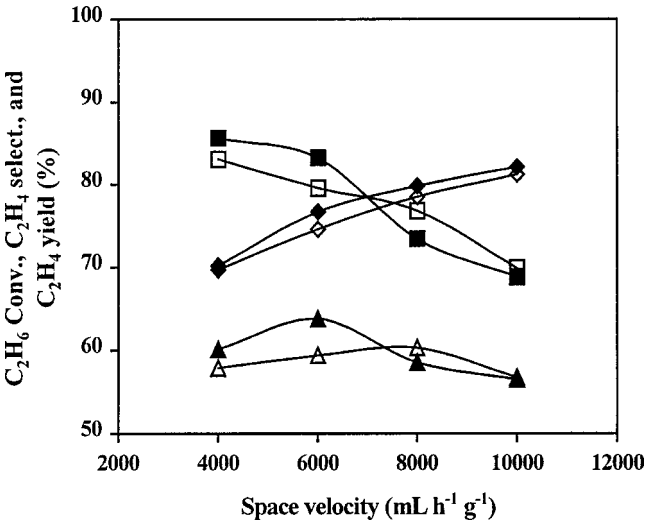

Figure 2. Effects of space velocity on catalytic performance of $La_{1.6}Sr_{0.4}CuO_{3.857}F_{0.143}$ (solid) and $La_{1.6}Sr_{0.4}CuO_{3.856}Cl_{0.126}$ (open) at 660 °C. (■, □) C_2H_6 conversion, (♦, ◇) C_2H_4 selectivity, (▲, △) C_2H_4 yield.

and CH_4 selectivity increased. At 660 °C, C_2H_4 selectivity reached a maximum value of 76.7% and the corresponding C_2H_6 and O_2 conversions, CH_4 and CO_x selectivities, and C_2H_4 yield were 83.2, 99.7, 3.1, 20.2, and 63.8%, respectively. Over the $La_{1.6}Sr_{0.4}CuO_{3.856}Cl_{0.126}$ catalyst, a similar trend was observed; the best catalytic performance was achieved at 660 °C, where C_2H_6 and O_2 conversions, C_2H_4 selectivity, CH_4 and CO_x selectivities, and C_2H_4 yield were 79.6, 98.8, 74.6, 2.3, 23.1, and 59.4%, respectively. The formation of CH_4 requires the breakage of the C–C bond. As suggested by Kennedy and Cant [39], methane generation follows two possible routes, i.e., ethane decomposition in the gas phase and a heterogeneous pathway involving an ethylperoxy intermediate. Ethylperoxy reacted with surface oxygen species to form CH_4 and HCO_2; the latter was further oxidized to CO_x. The increase in selectivity toward one of the products with the increase in reactant conversion is unusual in heterogeneous catalysis. In C_2H_6 oxidation at a particular O_2 conversion, C_2H_4 selectivity and C_2H_6 conversion can increase concurrently if deep oxidation is reduced. Based on these results, one can conclude that the $La_{1.6}Sr_{0.4}CuO_{4-\delta}X_\sigma$ catalyst is much superior to the $La_{1.6}Sr_{0.4}CuO_{3.852}$ catalyst in catalyzing the ODE reaction.

The influence of space velocity on catalytic performance is shown in figure 2. With the rise in space velocity from 4000 to 10000 ml h^{-1} g^{-1}, C_2H_6 conversion decreased whereas C_2H_4 selectivity increased, giving a maximum C_2H_4 yield of 63.8% for $La_{1.6}Sr_{0.4}CuO_{3.857}F_{0.143}$ at 6000 ml h^{-1} g^{-1} and of 60.3% for $La_{1.6}Sr_{0.4}CuO_{3.856}Cl_{0.126}$ at 8000 ml h^{-1} g^{-1}. Similar results were obtained when each of the two catalysts was well dispersed in quartz sand (0.5 g catalyst/5.0 g quartz sand). This indicates that the problem of hot spots was insignificant. We performed the lifetime studies in a period of 60 h of on-stream ODE reaction and the results manifest that the $La_{1.6}Sr_{0.4}CuO_{4-\delta}X_\sigma$ catalysts showed stable performance within the 60 h of reaction. As shown in table 1, the F or Cl contents and surface areas of the fresh and used (after 60 h of reaction) halide-incorporated catalysts were rather similar, confirming that the $La_{1.6}Sr_{0.4}CuO_{4-\delta}X_\sigma$ catalysts are durable. To investigate the reactivity of C_2H_4 towards O_2 over the three catalysts, we carried out C_2H_4 oxidation experiments under reaction conditions similar to those in C_2H_6 oxidation reaction at 660 °C, and the results are listed in table 2. One can observe that the C_2H_4 conversion was 12.2% over the F-doped catalyst and 13.9% over the Cl-doped catalyst whereas over $La_{1.6}Sr_{0.4}CuO_{3.852}$, it was 33.8%. Furthermore, the CO/CO_2 ratios in the product mixture obtained over $La_{1.6}Sr_{0.4}CuO_{4-\delta}X_\sigma$ were much higher than that obtained over $La_{1.6}Sr_{0.4}CuO_{3.852}$. As pointed out by Lunsford and co-workers [40], C_2H_4 was the major carbon source for CO_x formation at or above 650 °C. If C_2H_4 deep oxidation was reduced or suppressed, C_2H_4 selectivity would be enhanced. From the large differences in C_2H_4 selectivity and C_2H_6 conversion between the undoped and halide-doped catalysts, one can conclude that the introduction of F^- or Cl^- ions to $La_{1.6}Sr_{0.4}CuO_{4-\delta}$ resulted in the reduction of C_2H_4 deep oxidation.

Table 2
Catalytic performance of $La_{1.6}Sr_{0.4}CuO_{3.852}$, $La_{1.6}Sr_{0.4}CuO_{3.857}F_{0.143}$, and $La_{1.6}Sr_{0.4}CuO_{3.856}Cl_{0.126}$ for the oxidation of ethane and ethene at 660 °C and 6000 ml h^{-1} g^{-1}.

Catalyst	Oxidation of C_2H_4[a]		Oxidation of C_2H_6	
	C_2H_4 conversion (%)	CO/CO_2 ratio	C_2H_6 conversion (%)	C_2H_4 selectivity (%)
$La_{1.6}Sr_{0.4}CuO_{3.852}$	33.8	1/20.4	31.9	32.2
$La_{1.6}Sr_{0.4}CuO_{3.857}F_{0.143}$	12.2	1/3.7	83.2	76.7
$La_{1.6}Sr_{0.4}CuO_{3.856}Cl_{0.126}$	13.9	1/4.4	79.6	74.6

[a] At $C_2H_4/O_2/N_2$ molar ratio = 2/1/3.7.

3.2. Copper oxidation state, oxygen vacancy density, and halide location

For the $La_{1.6}Sr_{0.4}CuO_{3.857}F_{0.143}$ and $La_{1.6}Sr_{0.4}CuO_{3.856}Cl_{0.126}$ catalysts, the halide ions could (i) replace some of the O^{2-} ions, (ii) occupy oxygen vacancies or (iii) dwell at interstitial sites. If a F^- or Cl^- ion replaces an O^{2-} ion, to maintain electroneutrality, the oxidation state of an adjacent copper ion has to drop from Cu^{3+} to Cu^{2+}; if a halide ion occupies an oxygen vacancy or an interstitial position, it would cause the oxidation state of an adjacent copper ion to rise from Cu^{2+} to Cu^{3+}. From table 1, one may observe that the introduction of F^- or Cl^- ions into $La_{1.6}Sr_{0.4}CuO_{4-\delta}$ caused the Cu^{3+}/Cu ratios to increase rather than to decrease, demonstrating that the halide ions have occupied a certain amount of oxygen vacancies and/or interstitial spacings [19,41].

Summarized in table 3 are the changes in Cu^{3+}/Cu ratios in $La_{1.6}Sr_{0.4}CuO_{3.852}$, $La_{1.6}Sr_{0.4}CuO_{3.857}F_{0.143}$, and $La_{1.6}Sr_{0.4}CuO_{3.856}Cl_{0.126}$ under various thermal treatments; with a rise in temperature from 400 to 720 °C in a He atmosphere, the Cu^{3+}/Cu ratio decreased from 20.5 to

Table 3
Changes of Cu^{3+}/Cu ratios in $La_{1.6}Sr_{0.4}CuO_{3.852}$, $La_{1.6}Sr_{0.4}CuO_{3.857}F_{0.143}$, and $La_{1.6}Sr_{0.4}CuO_{3.856}Cl_{0.126}$ after thermal treatments in He at 400, 580, and 720 °C, respectively.

Catalyst	Cu^{3+}/Cu ratio[a] (mol%)			Halide content[b]	Weight loss due to the desorption of oxygen species[c] (wt%)		
	400 °C	580 °C	720 °C	800 °C (wt%)	400 °C	580 °C	720 °C
$La_{1.6}Sr_{0.4}CuO_{3.852}$	20.5 (20.7)	10.4 (20.5)	5.4 (20.6)	–	0	0.42	0.52
$La_{1.6}Sr_{0.4}CuO_{3.857}F_{0.143}$	25.6 (25.9)	25.3 (25.7)	0.3 (25.6)	0.70	0	0.01	0.53
$La_{1.6}Sr_{0.4}CuO_{3.856}Cl_{0.126}$	23.8 (23.6)	23.2 (23.7)	0.5 (23.9)	1.16	0	0.02	0.50

[a] Values in parentheses were obtained after the thermally treated sample was exposed to an oxygen flow of 20 ml min^{-1} at the same temperature for 30 min.
[b] Halide contents of the samples thermally treated in He at 800 °C for 30 min.
[c] Weight losses were estimated based on the changes in Cu^{3+}/Cu ratio.

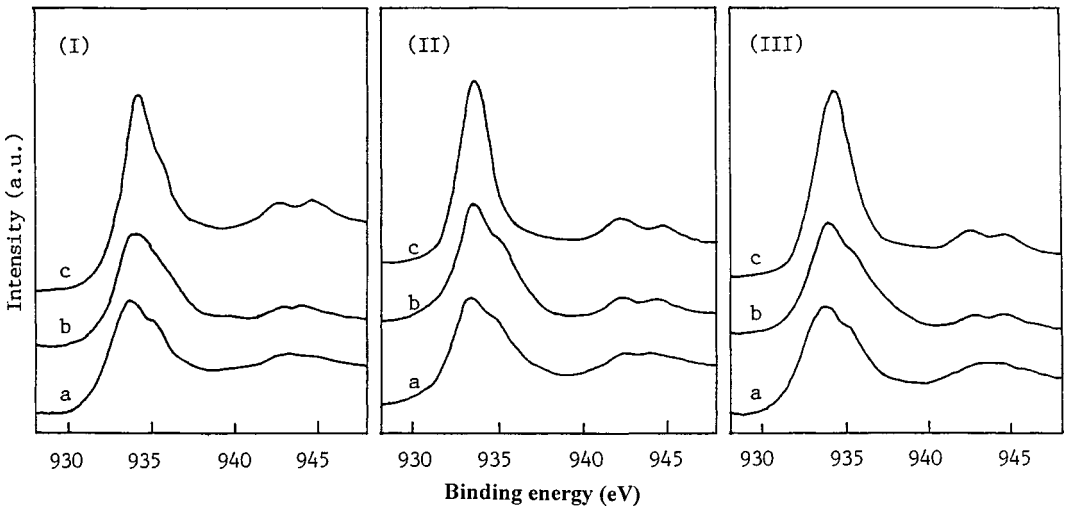

Figure 3. The Cu($2p_{3/2}$) spectra of (I) $La_{1.6}Sr_{0.4}CuO_{3.852}$, (II) $La_{1.6}Sr_{0.4}CuO_{3.857}F_{0.143}$, and (III) $La_{1.6}Sr_{0.4}CuO_{3.856}Cl_{0.126}$ treated in helium at (a) 400, (b) 580, and (c) 680 °C, respectively.

5.4 mol%, 25.6 to 0.3 mol%, and 23.8 to 0.5 mol%, respectively. It indicates that the abatement in Cu^{3+}/Cu ratio is induced by the desorption of oxygen species on/in the catalysts. Exposing the treated samples to an oxygen flow of 20 ml min^{-1} at the same temperature for 30 min restored the Cu^{3+}/Cu ratios to their former values (table 1), indicating that the Cu^{3+} amounts could be replenished by the oxidation of Cu^{2+}. There was no significant change in halide content when the catalysts were heated in He at 800 °C for 30 min. These results indicate that in an oxygen-deprived atmosphere, the drop in Cu^{3+}/Cu ratio is due to the desorption of oxygen species. Based on the Cu^{3+}/Cu ratios and the nature of oxygen desorption described below (figure 6), the weight losses due to the desorption of oxygen species were estimated and are listed in table 3.

The XPS spectra of Cu(2p) for $La_{1.6}Sr_{0.4}CuO_{3.852}$ and $La_{1.6}Sr_{0.4}CuO_{4-\delta}X_{\sigma}$ exhibited two main peaks corresponding to the $2p_{1/2}$ and $2p_{3/2}$ levels and shake-up satellites were observed ca. 10 eV from the main peaks. Figure 3 shows the Cu($2p_{3/2}$) spectra of the samples which had been treated in He at 400, 580, and 680 °C, respectively. One can observe that signal intensities of the shake-up satellite peaks increased with the rise in treatment temperature for the three catalysts. It might be associated with the increase in Cu^{2+} concentration due to the desorption of oxygen species at elevated temperatures. The shake-up satellites observed in the Cu($2p_{3/2}$) spectra (figure 3) were caused by charge transfer from neighbouring oxygen ligands into an empty d state of the Cu^{2+} ion [42]. The Cu($2p_{3/2}$) peaks of $La_{1.6}Sr_{0.4}CuO_{3.857}F_{0.143}$, $La_{1.6}Sr_{0.4}CuO_{3.856}Cl_{0.126}$, and $La_{1.6}Sr_{0.4}CuO_{3.852}$ were at ca. 933.5 eV. Since the binding energy of the 2p electron of a Cu^{3+} ion is larger than that of a Cu^{2+} ion (ca. 933.5 eV) or a Cu^{+} ion (ca. 932.7 eV) [43], another peak corresponding to Cu($2p_{3/2}$) = ca. 935 eV is expected to appear. From figure 3, one can observe a shoulder peak 934.9 eV, indicating the presence of Cu^{3+} in these catalysts; furthermore, the signal of Cu^{3+} ions decreased in intensity with the rise in temperature and disappeared at 680 °C, indicating that the concentration of Cu^{3+} ions decreased on heating in He for these three catalysts. The results of the analyses of copper oxidation state support the assignment. A similar Cu($2p_{3/2}$) feature has been

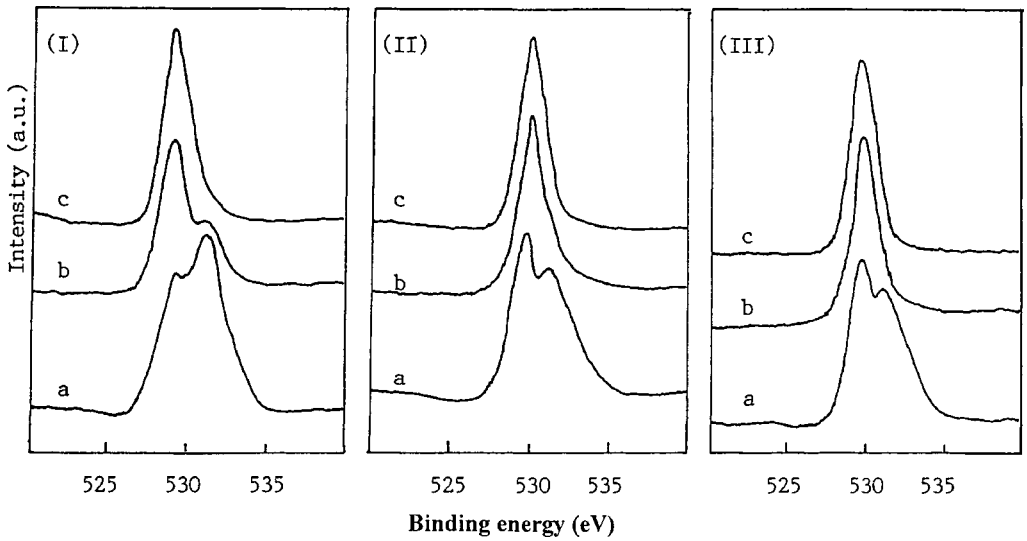

Figure 4. The O(1s) spectra of (I) $La_{1.6}Sr_{0.4}CuO_{3.852}$, (II) $La_{1.6}Sr_{0.4}CuO_{3.857}F_{0.143}$, and (III) $La_{1.6}Sr_{0.4}CuO_{3.856}Cl_{0.126}$ treated in helium at (a) 400, (b) 580, and (c) 680 °C, respectively.

reported by Ospett et al. [44] and Soderholm et al. [45], who confirmed the existence of trivalent copper ions in a $La_{1.85}Sr_{0.15}CuO_{4-\delta}$ sample by using chemical analysis and X-ray absorption spectroscopic studies. The negative results in Cu^+ analysis and the absence of signals due to Cu^+ ions in XPS analysis exclude the presence of Cu^+ in these samples. The above results confirm that there are only Cu^{2+} and Cu^{3+} ions in $La_{1.6}Sr_{0.4}CuO_{4-\delta}$ and $La_{1.6}Sr_{0.4}CuO_{4-\delta}X_\sigma$.

The O(1s) XPS spectra of the $La_{1.6}Sr_{0.4}CuO_{3.852}$, $La_{1.6}Sr_{0.4}CuO_{3.857}F_{0.143}$, and $La_{1.6}Sr_{0.4}CuO_{3.856}Cl_{0.126}$ samples treated in He at 400, 580, and 680 °C, respectively, are shown in figure 4. There are two O(1s) peaks at ca. 529 and 531 eV (binding energy) for the three samples treated at 400 °C. We assign the signal at lower binding energy to surface lattice oxygen and the one at higher binding energy to adsorbed oxygen species such as O^- [46–49]. The O(1s) binding energy of OH^- falls in the 531–532 eV range. In order to eliminate the possibility of OH^- presence, we had heated the samples in an O_2 flow at 800 °C for 1 h before the XPS measurement. There is only one O(1s) peak at 530.3 eV for the $La_{1.6}Sr_{0.4}CuO_{3.857}F_{0.143}$ sample and one O(1s) peak at 529.9 eV for the $La_{1.6}Sr_{0.4}CuO_{3.856}Cl_{0.126}$ sample treated in He at 580 and 680 °C (figure 4 (II) and (III), spectra (b) and (c)); these could be assigned to surface lattice oxygen [46–49]. As for a halogen-free $La_{1.6}Sr_{0.4}CuO_{3.852}$ sample, with the rise of treatment temperature, the component at 531.4 eV decreased markedly in intensity and disappeared after treatment at 680 °C whereas the intensity of the component at 529.3 eV increased (figure 4(I), spectra (a)–(c)). From the O(1s) spectra, one can observe that the O(1s) binding energy of the lattice oxygen in $La_{1.6}Sr_{0.4}CuO_{3.857}F_{0.143}$ (530.3 eV) and $La_{1.6}Sr_{0.4}CuO_{3.856}Cl_{0.126}$ (529.9 eV) was 0.6–1.0 eV higher than that (529.3 eV) in $La_{1.6}Sr_{0.4}CuO_{3.852}$. Due to the electronegativity of F (3.98) and Cl (3.16) [50], the inclusion of F or Cl in $La_{1.6}Sr_{0.4}CuO_{4-\delta}$ would cause the valence electron density of O^{2-} to decrease and the O(1s) binding energy of O^{2-} to rise. It means that the presence of F or Cl in the tetragonal K_2NiF_4-type lattice would weaken the copper−oxygen bonds. Taking into account the fact that the O^{2-} (radius, 1.40 Å [51]) and F^- (radius, 1.38 Å [51]) ions are similar in size whereas the Cl^- (radius, 1.81 Å [51]) ions are somewhat larger than the O^{2-} ions, the F^- ions would enter into the $La_{1.6}Sr_{0.4}CuO_{4-\delta}$ lattice more readily than the Cl^- ions and the embedding of Cl^- ions would induce the enlargement of the $La_{1.6}Sr_{0.4}CuO_{4-\delta}$ lattice. Based on the XRD results, the tetragonal lattice parameters, a and c, were estimated to be, respectively, 3.7756 and 13.1924 Å for $La_{1.6}Sr_{0.4}CuO_{3.852}$ and 3.8702 and 13.0951 Å for $La_{1.6}Sr_{0.4}CuO_{3.856}Cl_{0.126}$ (the lattice constants were calculated using a standard least-squares refinement method). That means that the introduction of Cl^- ions would weaken the coulombic force between a copper ion and an O^{2-} ion. As a result, lattice O^{2-} would become more mobile. In other words, the inclusion of F^- or Cl^- ions in $La_{1.6}Sr_{0.4}CuO_{4-\delta}$ enhances the mobility of lattice oxygen. The increase in C_2H_4 selectivity over the halide-doped $La_{1.6}Sr_{0.4}CuO_{4-\delta}X_\sigma$ catalysts (figure 1 (b) and (c)) is supporting evidence for this viewpoint.

The pioneering work of Ovshinsky et al. [52] has given impetus to the investigation of the consequences of anion isomorphism in HTSCs. It is important to confirm the presence and location of halogen atoms in the crystal lattice. Works on fluorinated $YBa_2Cu_3O_{7-\delta}$ [53–56] manifest that the incorporated halogen atoms occupy the vacant oxygen positions in the Cu(1) plane where the Cu^{3+} ion is also located [57]. Figure 5 shows the crystal structure of $La_{2-x}Sr_xCuO_4$ (T-structure). This unit cell contains two-dimensional sheets of Cu–O octahedra; there are two kinds of oxygen atoms (O(1) – apical oxygen and O(2)) as indicated in figure 5. Oxygen vacancies could be present at both O(1) and O(2) sites [58]. The observations of Al-Mamouri et al. [59] and a Madelung energy calculation [60] reveal

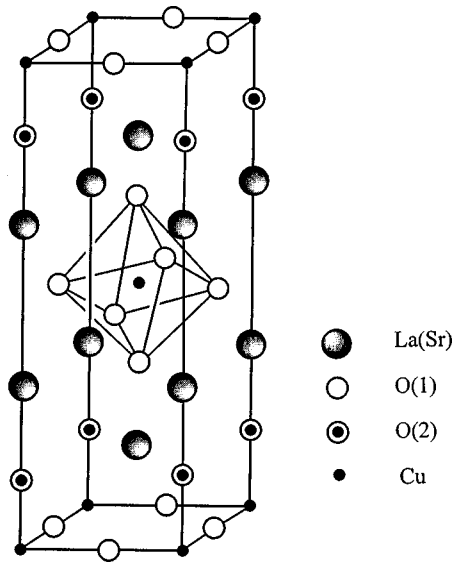

Figure 5. The crystal structure of $La_{2-x}Sr_xCuO_4$ (T-structure).

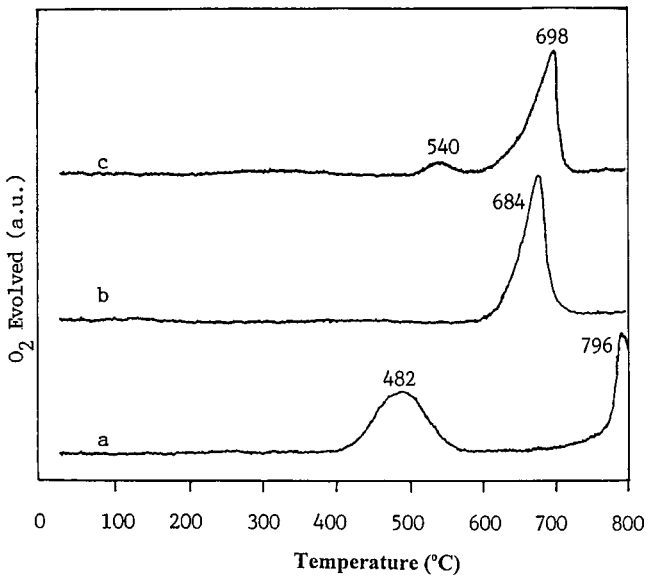

Figure 6. The O_2-TPD profiles of (a) $La_{1.6}Sr_{0.4}CuO_{3.852}$, (b) $La_{1.6}Sr_{0.4}CuO_{3.857}F_{0.143}$, and (c) $La_{1.6}Sr_{0.4}CuO_{3.856}Cl_{0.126}$.

that F^- ions preferably occupy the apical sites (O(1)). In addition, F^- ions can also enter into the interstitial sites (0, 1/2, 1/4) as reported in $Sr_2CuO_2F_{2+\delta}$ [59]. The occupation of O(1) sites by the doped halide ions has been confirmed by Chen et al., who investigated a $La_{0.7}Sr_{1.3}Cu(O,F)_{4+\delta}$ HTSC material [24]. By determining the lattice parameters of $Nd_2CuO_{4-x}F_x$, James et al. [61] pointed out that the doped fluoride ions were located at the O(2) sites around the Nd^{3+} ions. However, Sugiyama et al. [62] considered that there is a possibility that the doped F^- ions occupy both the O(1) and O(2) sites. In the case of $La_{1.6}Sr_{0.4}CuO_{4-\delta}X_\sigma$, the generation of Cu^{3+} ions would be induced by the preferential occupation of the originally vacant O(1) sites by X^- ions. In other words, the incorporated X^- ions dwelt at the O(1) sites in the CuO_6 octahedral plane, forcing the oxidation state of the nearest copper ion to rise.

3.3. Active oxygen species

By determining the exact oxygen composition of $La_{1-x}Sr_xCoO_{3-\delta}$ ($x = 0$–1) before and after the respective desorption peaks, Yamazoe et al. pointed out that a certain amount of Co^{4+} ion was actually induced by the oxygen dissociatively adsorbed at oxygen vacancies [48]. Generally speaking, only after calcination in an O_2-containing atmosphere would the oxygen vacancies in a catalyst be occupied by dissociatively adsorbed oxygen (O^-). In the calcined $La_{1.6}Sr_{0.4}CuO_{4-\delta}$ catalysts, some Cu^{3+} ions were formed due to the occupancy of oxygen vacancies by O^-. Rao [63] pointed out that there were O^- species settling in the oxygen holes in $YBa_2Cu_3O_{7-\delta}$. The detection of the signal at ca. 531 eV O(1s) binding energy (figure 4(I)) indicates the presence of O^- in the $La_{1.6}Sr_{0.4}CuO_{3.852}$ catalyst. These results demonstrate that there were O^- species accommodated in the oxygen vacancies of the undoped catalyst, driving the Cu^{3+} content to rise. Due to the fact that the halogenation process of $La_{1.6}Sr_{0.4}CuO_{4-\delta}$ was carried out in vacuum (0.1 Torr), it is understandable that the O^- signal observed on the F- or Cl-doped catalyst treated in He at temperatures varied from 400 to 680 °C was weak or undetectable (figure 4 (II) and (III), spectra (a)–(c)).

Both α and β oxygen desorptions in O_2-TPD profile are characteristics of most perovskites. The α oxygen is accommodated in oxygen vacancies [48,63–65] and is responsible for the complete oxidation of hydrocarbons; the desorption of β oxygen (i.e., lattice oxygen) is attributed to the partial reduction of a B-site cation by lattice oxygen and is responsible for the selective oxidation of hydrocarbons [64,65]. The inclusion of F^- or Cl^- ions in the $La_{1.6}Sr_{0.4}CuO_{4-\delta}$ lattice would induce two effects: (i) the decrease in the amount of oxygen vacancies, i.e., the decrease of α oxygen; (ii) the rise in Cu^{3+}/Cu ratio, i.e., the increase of β oxygen (ascribable to the partial reduction of copper from 3+ to 2+ or even to 1+) desorption. As shown in table 1, the introduction of F^- or Cl^- ions into $La_{1.6}Sr_{0.4}CuO_{4-\delta}$ led to the increase rather than the decrease in Cu^{3+}/Cu ratio. This indicates that the F^- or Cl^- ions have occupied a certain amount of oxygen vacancies and/or interstitial sites. Figure 6 shows the O_2-TPD profiles of $La_{1.6}Sr_{0.4}CuO_{3.852}$ and $La_{1.6}Sr_{0.4}CuO_{4-\delta}X_\sigma$. There are two desorption peaks in the $La_{1.6}Sr_{0.4}CuO_{3.852}$ (figure 6(a)) and $La_{1.6}Sr_{0.4}CuO_{3.856}Cl_{0.126}$ (figure 6(c)) profiles. According to the nature of desorbed oxygen, the peak at ca. 482 °C (135.4 μmol g_{cat}^{-1}) or 540 °C (9.8 μmol g_{cat}^{-1}) can be assigned to α oxygen, whereas the one at ca. 698 °C (156.2 μmol g_{cat}^{-1}) or 796 °C to β oxygen. In the $La_{1.6}Sr_{0.4}CuO_{3.857}F_{0.143}$ profile (figure 6(b)), however, there is only one peak at ca. 684 °C, which can be assigned to β oxygen; the corresponding amount of desorbed oxygen was 170.1 μmol g_{cat}^{-1}. The results of O_2-TPD studies clearly indicate that with the addition of F^- or Cl^- ions to $La_{1.6}Sr_{0.4}CuO_{4-\delta}$, the content of α oxygen

Table 4
TGA results of $La_{1.6}Sr_{0.4}CuO_{3.852}$, $La_{1.6}Sr_{0.4}CuO_{3.857}F_{0.143}$, and $La_{1.6}Sr_{0.4}CuO_{3.856}Cl_{0.126}$.

Catalyst	Temperature range (°C)	Weight loss (wt%)
$La_{1.6}Sr_{0.4}CuO_{3.852}$	25–580	0.46
	580–720	0.11
$La_{1.6}Sr_{0.4}CuO_{3.857}F_{0.143}$	25–580	0
	580–720	0.56
$La_{1.6}Sr_{0.4}CuO_{3.856}Cl_{0.126}$	25–580	0.02
	580–720	0.51

decreased (for $La_{1.6}Sr_{0.4}CuO_{3.857}F_{0.143}$, the α oxygen disappeared) whereas that of β oxygen increased; furthermore, the desorption temperature of the β oxygen was obviously lowered. Therefore, we suggest that the incorporation of F^- or Cl^- ions into the $La_{1.6}Sr_{0.4}CuO_{4-\delta}$ lattice has caused the bulk oxygen vacancy density to decrease, and so the complete oxidation reactions were reduced as a result.

Table 4 summarizes the results of TGA experiments. The weight losses of the catalysts occurred in two temperature ranges: 25–580 and 580−720 °C. The amount of weight loss in the former temperature range is much larger for $La_{1.6}Sr_{0.4}CuO_{3.857}$ than that for $La_{1.6}Sr_{0.4}CuO_{3.857}F_{0.143}$ or $La_{1.6}Sr_{0.4}CuO_{3.856}Cl_{0.126}$; in the latter temperature range, however, the amounts of weight loss observed over the two halide-doped catalysts are much more than that of the undoped one. As halide leaching was insignificant (tables 1 and 3), we consider that the weight losses observed in the TGA studies were due to the desorption of oxygen species via two steps:

$$Cu^{3+} + O^-_{vacancy} \xrightarrow{\alpha\ \text{oxygen}} Cu^{2+} + \tfrac{1}{2}O_2 \qquad (1)$$

$$2Cu^{3+} + O^{2-}_{lattice} \xrightarrow{\beta\ \text{oxygen}} 2Cu^{2+} + \tfrac{1}{2}O_2 \qquad (2)$$

From table 4, one may ascribe the weight losses below 580 °C over these catalysts to the desorption of α oxygen [10] via equation (1) and those between 580 and 720 °C to the desorption of lattice (β) oxygen [66] via equation (2). For all the catalysts, the weight losses were rather close to those due to the desorption of dissociatively adsorbed oxygen located in oxygen vacancies (all the oxygen vacancies were presumably occupied by dissociatively adsorbed oxygen) below 580 °C whereas between 580 and 720 °C, the weight loss values were less than those estimated based on partial Cu^{3+} reduction. For the halogenated catalysts, the amounts of desorbed α oxygen decreased or even disappeared whereas those of β oxygen increased compared to the halide-free catalyst. It indicates that the addition of halide ions promoted the mobility of lattice oxygen. It can be observed that the $La_{1.6}Sr_{0.4}CuO_{3.857}F_{0.143}$ and $La_{1.6}Sr_{0.4}CuO_{3.856}Cl_{0.126}$ catalysts had similar weight losses in the two temperature ranges. Obviously, the weight losses in the halo-oxide catalysts were quite close to the estimated values, whereas for the undoped catalyst, although a weight loss of 0.46 wt% below 580 °C agreed with the predicted value of α oxygen, a weight loss of 0.11 wt% between 580 and 720 °C was much less than the predicted figure (0.22 wt%) of β oxygen, indicating that the lattice oxygen in $La_{1.6}Sr_{0.4}CuO_{3.852}$ was much less mobile than those in $La_{1.6}Sr_{0.4}CuO_{3.857}F_{0.143}$ and $La_{1.6}Sr_{0.4}CuO_{3.856}Cl_{0.126}$. From table 3, one can observe that in a He atmosphere, most of the dissociatively adsorbed oxygen species in $La_{1.6}Sr_{0.4}CuO_{3.852}$ desorbed at 580 °C, resulting in a weight loss of 0.42 wt%, a value rather close to the theoretical value (0.45 wt%) of equation (1); and there was a noticeable decrease in Cu^{3+} content. Between 580 and 720 °C, the Cu^{3+} content decreased by ca. 48% and the weight loss was 0.11 wt%. The results indicate that a large extent of weight loss was due to the desorption of α oxygen and the lattice oxygen was not mobile in $La_{1.6}Sr_{0.4}CuO_{3.852}$. As for $La_{1.6}Sr_{0.4}CuO_{3.857}F_{0.143}$ and $La_{1.6}Sr_{0.4}CuO_{3.856}Cl_{0.126}$, however, with the rise in treatment temperature, the decreases in Cu^{3+} content were significant and the weight losses of 0.56 and 0.51 wt% were getting close to the expected values (0.52 and 0.48 wt%) of equation (2), respectively. The results indicate that the introduction of F^- or Cl^- ions into $La_{1.6}Sr_{0.4}CuO_{4-\delta}$ enhanced the mobility of lattice oxygen. Passing oxygen (20 ml min^{-1}) through the catalysts which had just been thermally treated in He would restore the Cu^{3+} contents to the former values (table 1). The results demonstrate that the oxygen consumed in the ODE reaction could be replen-

Table 5
Catalytic performances of $La_{1.6}Sr_{0.4}CuO_{3.852}$, $La_{1.6}Sr_{0.4}CuO_{3.857}F_{0.143}$, and $La_{1.6}Sr_{0.4}CuO_{3.856}Cl_{0.126}$ in a C_2H_6 or $C_2H_6/O_2/N_2$ pulse after thermal treatment in He, respectively, at 480, 540, 660, and 720 °C for 30 min.[a]

Catalyst	480 °C[b]		540 °C[b]		660 °C[b]		720 °C[b]	
	C_2H_6 conversion (%)	C_2H_4 selectivity (%)	C_2H_6 conversion (%)	C_2H_4 selectivity (%)	C_2H_6 conversion (%)	C_2H_4 selectivity (%)	C_2H_6 conversion (%)	C_2H_4 selectivity (%)
$La_{1.6}Sr_{0.4}CuO_{3.852}$	14.1	6.2	14.3	22.6	35.8	41.7	55.4	82.9
	(15.6)	(4.1)	(17.8)	(21.2)	(37.3)	(44.6)	(66.8)	(75.1)
$La_{1.6}Sr_{0.4}CuO_{3.857}F_{0.143}$	7.6	26.3	38.2	37.9	83.4	85.6	88.8	91.7
	(9.3)	(28.8)	(40.6)	(40.1)	(84.2)	(83.9)	(90.9)	(88.5)
$La_{1.6}Sr_{0.4}CuO_{3.856}Cl_{0.126}$	8.2	27.6	33.6	36.5	80.5	83.8	86.7	92.8
	(8.6)	(28.3)	(39.9)	(39.7)	(82.8)	(82.2)	(90.1)	(87.9)

[a] Upper values in a pulse of C_2H_6. The values in parentheses were obtained in a pulse of $C_2H_6/O_2/N_2$ (molar ratio = 2/1/3.7).

[b] Temperature for thermal treatment and reactant pulsing.

ished by the oxygen from the gas phase according to the sequence

$$O_2(g) \leftrightarrow O_2^-(ads) \leftrightarrow O_2^{2-}(ads) \leftrightarrow 2O^-(ads)$$
$$\leftrightarrow 2O^{2-}(ads) \leftrightarrow 2O^{2-}_{lattice}$$

When the treatment temperature was raised from 580 to 720 °C, with the removal of lattice oxygen from these three catalysts due to the partial reduction of Cu^{3+} ions, the oxygen vacancy density increased. The rise in oxygen vacancy density is favourable for the transformation of gaseous oxygen to lattice oxygen; as a result, the loss induced by Cu^{3+} reduction is compensated.

Table 5 summarizes the C_2H_6 conversions and C_2H_4 selectivities when the thermally treated $La_{1.6}Sr_{0.4}CuO_{3.852}$, $La_{1.6}Sr_{0.4}CuO_{3.857}F_{0.143}$, and $La_{1.6}Sr_{0.4}CuO_{3.856}Cl_{0.126}$ samples were exposed, respectively, to a C_2H_6 or $C_2H_6/O_2/N_2$ (molar ratio = 2/1/3.7) pulse at the temperature of thermal treatment. In both cases of pulsing C_2H_6 and pulsing $C_2H_6/O_2/N_2$, with a rise in treatment temperature from 480 to 720 °C, C_2H_4 selectivity and C_2H_6 conversion increased significantly over the three catalysts. When a C_2H_6 pulse was introduced, respectively, to the three catalysts at 480 °C, $La_{1.6}Sr_{0.4}CuO_{3.852}$ showed the highest C_2H_6 conversion but poorest C_2H_4 selectivity, confirming that α oxygen is responsible for the complete oxidation of C_2H_6 and C_2H_4. At 580 or 720 °C, C_2H_6 conversion and C_2H_4 selectivity recorded in a pulse of C_2H_6 or in a pulse of $C_2H_6/O_2/N_2$ increased significantly over the three catalysts, indicating that the β oxygen (i.e., lattice oxygen) is accountable for the selective oxidation of C_2H_6 to C_2H_4. Considering the nature and functions of oxygen species on/in the $La_{1.6}Sr_{0.4}CuO_{3.852}$, $La_{1.6}Sr_{0.4}CuO_{3.857}F_{0.143}$, and $La_{1.6}Sr_{0.4}CuO_{3.856}Cl_{0.126}$ catalysts, it is clear that the α oxygen is prone to induce ethane deep oxidation whereas the β oxygen is responsible for ethane selective oxidation to ethene.

4. Conclusions

Based on the above results and discussion, we conclude that (i) the halogenated $La_{1.6}Sr_{0.4}CuO_{4-\delta}$ catalysts have a tetragonal perovskite-related structure; (ii) the addition of fluoride or chloride ions to the $La_{1.6}Sr_{0.4}CuO_{4-\delta}$ lattice significantly enhanced C_2H_4 selectivity and C_2H_6 conversion; (iii) the inclusion of halide ions in the $La_{1.6}Sr_{0.4}CuO_{4-\delta}$ lattice could promote lattice oxygen mobility; (iv) the monoxygen (O^-) species desorbed below 600 °C induce total oxidation whereas the lattice oxygen species desorbed within the 600–700 °C range favor selective oxidation of C_2H_6 to C_2H_4; and (v) the good and sustainable catalytic behavior of the F- or Cl-doped perovskite-related oxide catalysts could be associated with the decrease in oxygen vacancy density and the rise in Cu^{3+}/Cu ratio.

Acknowledgement

The work described above was fully supported by a grant from the Research Grants Council of the Hong Kong Special Administration Region, PR China (Project No. HKBU 2015/99P). HXD thanks the HKBU for a Ph.D. studentship.

References

[1] S.J. Conway, D.J. Wang and J.H. Lunsford, Appl. Catal. A 79 (1991) L1.
[2] J.H. McCain, US Patent 4 524 236 (1985).
[3] S.B. Wang, K. Murata, T. Hayakawa, S. Hamakawa and K. Suzuki, Catal. Lett. 59 (1999) 173.
[4] W. Ueda, S.W. Lin and I. Tohmoto, Catal. Lett. 44 (1996) 241.
[5] K. Omata, O. Yamazaki, K. Tomita and K. Fujimoto, J. Chem. Soc. Chem. Commun. (1994) 1647.
[6] Y.S. Lin and Y. Zeng, J. Catal. 164 (1996) 220.
[7] T. Nozaki and K. Fujimoto, AIChE J. 40 (1994) 870.
[8] J.E. ten Helshof, H.J.M. Bouwmeester and H. Verweeij, Appl. Catal. A 130 (1995) 195.
[9] G.H. Yi, T. Hayakawa, A.G. Anderson, K. Suzuki, S. Hamakawa, A.P.E. York, M. Shimizu and K. Takehira, Catal. Lett. 38 (1996) 189.
[10] T. Seiyama, in: *Properties and Application of Perovskite-Type Oxides*, eds. L.G. Tejuca and J.L.G. Fierro (Dekker, New York, 1993) p. 215.
[11] B. Viswanathan, in: *Properties and Application of Perovskite-Type Oxides*, eds. L.G. Tejuca and J.L.G. Fierro (Dekker, New York, 1993) p. 271.
[12] H.X. Dai, C.F. Ng and C.T. Au, J. Catal. 189 (2000) 52.
[13] H.X. Dai, C.F. Ng and C.T. Au, Catal. Lett. 57 (1999) 115.
[14] J.G. Bednorz and K.A. Müller, Z. Phys. 64 (1986) 189.
[15] R.J. Cava, R.B. van Dover, B. Batlogg and E.A. Rietman, Phys. Rev. Lett. 58 (1987) 408.
[16] E.E. Alp, G.K. Shenoy, D.G. Hinks, D.W. Capone II, L. Soderholm and H.B. Schuttler, Phys. Rev. B 35 (1987) 7199.
[17] B.M. Tissue, K.M. Cirillo, J.C. Wright, M. Daeumling and D.C. Larbalestier, Solid State Commun. 65 (1988) 51.
[18] B. Chevalier, A. Tressaud, B. Lepine, K. Amine, J.M. Dance, L. Lozano, E. Hickey and J. Etourneau, Physica C 167 (1990) 97.
[19] V. Bhat, C.N.R. Rao and J.M. Honig, Solid State Commun. 81 (1992) 751.
[20] M.H. Tuilier, B. Chevalier, A. Tressaud, C. Brisson, J.L. Soubeyroux and J. Etourneau, Physica C 200 (1992) 113.
[21] C. Robin-Brisson, A. Tressaud, B. Chevalier, E. Ben Salem, J. Hejtmanek, J. Etourneau, M. Cassart and J.P. Issi, J. Alloys Compd. 188 (1992) 69.
[22] V. Bhat and J.M. Honig, Mater. Res. Bull. 30 (1995) 1253.
[23] S. Adachi, X.J. Wu, T. Tamura, T. Tatsuki, A. Tokiwa-Yamamoto and K. Tanabe, Physica C 291 (1997) 59.
[24] X. Chen, J. Liang, W. Tang, C. Wang and G. Rao, Phys. Rev. B 52 (1995) 16233.
[25] J.D. Jorgensen, H.B. Schuttler, D.G. Hinks, D.W. Capone II, K. Zhang, M.B. Brodsky and D.J. Scalapino, Phys. Rev. Lett. 58 (1987) 1024.
[26] E.H. Appelman, L.R. Morss, A.M. Kini, U. Geiser, A. Umezawa, G.W. Crabtree and K.D. Carlson, Inorg. Chem. 26 (1987) 3237.
[27] J.D. Jorgensen, B. Dabrowski, S. Pei, D.G. Hinks, L. Soderholm, B. Morosin, J.E. Schirber, E.L. Venturi and D.S. Ginley, Phys. Rev. B 38 (1988) 11337.
[28] V.I. Simonov, L.A. Muradyan, R.A. Tamazyan, V.V. Osiko, V.M. Tatarintsev and K. Gamayunov, Physica C 169 (1990) 123.
[29] J. Christopher and C.S. Swamy, J. Mol. Catal. 62 (1990) 69.
[30] S. Subramanian and C.S. Swamy, Catal. Lett. 35 (1995) 361.

[31] N. Nguyen, F. Studer and B. Raveau, J. Phys. Chem. Solids 44 (1983) 389.
[32] S. Rajadurai, J.J. Carberry, B. Li and C.B. Alcock, J. Catal. 131 (1991) 582.
[33] M.L. Rojas, J.L.G. Fierro, L.G. Tejuca and A.T. Bell, J. Catal. 124 (1990) 41.
[34] U. Asaf, I. Felner and U. Yaron, Physica C 211 (1993) 45.
[35] C.T. Au, Y.W. Liu and C.F. Ng, J. Catal. 176 (1998) 365.
[36] M. Oku, J. Kimura, M. Hosoya, K. Takada and K. Hirokawa, Fresenius Z. Anal. Chem. 332 (1988) 237.
[37] Y. Saito, T. Noji, K. Hirokawa, A. Endo, N. Matsuzaki, M. Katsumata and N. Higuchi, Jpn. J. Appl. Phys. 26 (1987) L838.
[38] N. Nguyen, J. Chiosnet, M. Hervieu and B. Raveau, J. Solid State Chem. 39 (1981) 120.
[39] E.M. Kennedy and N.W. Cant, Appl. Catal. 75 (1991) 321.
[40] C. Shi, M.P. Rosynek and J.H. Lunsford, J. Phys. Chem. 98 (1994) 8371.
[41] T. Tatsuki, S. Adachi, T. Tamura and K. Tanabe, Physica C 303 (1998) 41.
[42] K.S. Kim, J. Electron. Spectrosc. 3 (1974) 217.
[43] J.S. Shin, H. Enomoto, H. Takauchi, Y. Takno, N. Mori and H. Ozaki, Jpn. J. Appl. Phys. 28 (1989) L1365.
[44] M. Ospett, J. Henz, E. Kaldis and P. Wachter, Physica C 153–155 (1988) 159.
[45] L. Soderholm, E.E. Alp, M.A. Beno, L.R. Morss, G. Shenoy and G.L. Goodman, in: *High Temperature Superconductivity Materials*, eds. W.E. Hatfield and J.H. Miller, Jr. (Dekker, New York, 1988).
[46] G.U. Kulkarni, C.N.R. Rao and M.W. Roberts, J. Phys. Chem. 99 (1995) 3310.
[47] A.F. Carley, M.W. Roberts and A.K. Santra, J. Phys. Chem. B 101 (1997) 9978.
[48] N. Yamazoe, Y. Teraoka and T. Seiyama, Chem. Lett. (1981) 1767.
[49] J.L.G. Fierro and L.G. Tejuca, Appl. Surf. Sci. 27 (1987) 453.
[50] F.A. Cotton and G. Wilkinson, *Advanced Inorganic Chemistry*, 3rd Ed. (Interscience, New York, 1972).
[51] D.R. Lide, ed., *Handbook of Chemistry and Physics* (CRC Press, New York, 1998/1999).
[52] S.R. Ovshinsky, R.T. Young, D.D. Allred, G. Demaggio and G.A. van der Leeden, Phys. Rev. Lett. 58 (1987) 2579.
[53] J.R. LaGraff, E.C. Behrman, J.A.T. Taylor, E.J. Rotella, J.D. Jorgensen, L.Q. Wang and P.G. Mattocks, Phys. Rev. B 39 (1989) 347.
[54] C. Perrin, A. Dinia, O. Pena, M. Sergent, P. Burlet and J. Rossat-Mignod, Solid State Commun. 76 (1990) 401.
[55] A.P. Nemudry, Y.T. Pavlyukhin, N.G. Khainovskii and V.V. Boldyrev, Superconductivity 3 (1990) 1528 (in Russian).
[56] Yu.A. Ossipyan, O.V. Zharikov, G.Yu. Logvenov, N.S. Sidorov, V.I. Kulakov, I.M. Shmytko, I.K. Bdikin and A.M. Gromov, Physica C 165 (1990) 107.
[57] W.I.F. David, W.T.A. Harrison, J.M.F. Gunn, O. Moze, A.K. Soper, P. Day, J.D. Jorgensen, D.G. Hinks, M.A. Beno, L. Soderholm, D.W. Capone II, I.K. Schuller, C.U. Segre, K. Zhang and J.D. Grace, Nature 327 (1987) 310.
[58] F. Izumi, Y. Matsui, H. Takagi, Y. Tokura and H. Asano, Physica C 158 (1989) 433.
[59] M. Al-Mamouri, P.P. Edwards, C. Greaves and M. Slaski, Nature 369 (1994) 382.
[60] J.W. Weenk and H.A.T. Harwig, Phys. Chem. Solids 38 (1977) 1047.
[61] A.C.W.P. James, S.M. Zahurak and D.W. Murphy, Nature 338 (1989) 240.
[62] J. Sugiyama, M. Kosuge, Y. Ojima, H. Yamauchi and S. Tanaka, Physica C 179 (1991) 131.
[63] C.N.R. Rao, in: *Chemistry of Oxide Superconductivity*, ed. C.N.R. Rao (Blackwell, Oxford, 1988).
[64] A. Bielañski and J. Haber, *Oxygen in Catalysis* (Dekker, New York, 1991).
[65] J. Haber, in: *Surface Properties and Catalysis by Non-Metals*, eds. J.P. Bonnelle, B. Delmon and E. Derouane (Reidel, Dordrecht, 1983).
[66] Y. Wu, T. Yu, B.S. Dou, C.X. Wang, X.F. Xie, Z.L. Yu, S.R. Fan, Z.R. Fan and L.C. Wang, J. Catal. 120 (1989) 88.